LA-UR- 96-1325

CONF-960194--1

Title: LSND Neutrino Oscillation Results

Author(s): W. C. Louis

Submitted to: *International Conference on Orbis Scientiae 1996*
Miami, Florida
January 25–28, 1996

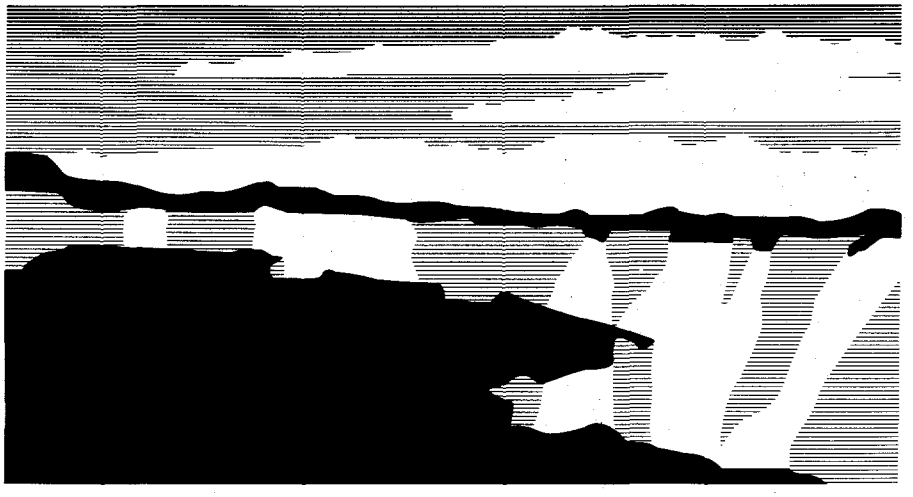

Los Alamos
NATIONAL LABORATORY

Form No. 836 R5
ST 2629 10/91

LSND NEUTRINO OSCILLATION RESULTS

W. C. Louis, representing the LSND Collaboration[1]

Los Alamos National Laboratory
Physics Division
Los Alamos, NM 87545, U.S.A.

INTRODUCTION

In the past several years, a number of experiments have searched for neutrino oscillations, where a neutrino of one type (say $\bar{\nu}_\mu$) spontaneously transforms into a neutrino of another type (say $\bar{\nu}_e$). For this phenomenon to occur, neutrinos must be massive and the apparent conservation law of lepton families must be violated. In 1995 the LSND experiment published data showing candidate events that are consistent with $\bar{\nu}_\mu \rightarrow \bar{\nu}_e$ oscillations.[2] Additional data are reported here which provide stronger evidence for neutrino oscillations.[3]

THE LSND EXPERIMENT

The Liquid Scintillator Neutrino Detector (LSND) experiment at LAMPF [3] is designed to search with high sensitivity for $\bar{\nu}_\mu \rightarrow \bar{\nu}_e$ oscillations from μ^+ decay at rest. LAMPF is a most intense source of low energy neutrinos due to its 1 mA proton intensity and 800 MeV energy. The neutrino source is well understood because almost all neutrinos arise from π^+ or μ^+ decay; π^- and μ^- are readily captured in the Fe of the shielding and Cu of the beam stop. The production of kaons and heavier mesons is negligible at these energies. The $\bar{\nu}_e$ rate is calculated to be only 4×10^{-4} relative to $\bar{\nu}_\mu$ in the $36 < E_\nu < 52.8$ MeV energy range, so that the observation of a significant $\bar{\nu}_e$ rate would be evidence for $\bar{\nu}_\mu \rightarrow \bar{\nu}_e$ oscillations.

The LSND detector consists of an approximately cylindrical tank 8.3 m long by 5.7 m in diameter. The center of the detector is 30 m from the neutrino source. On the inside surface of the tank 1220 8-inch Hammamatsu phototubes provide 25% photocathode coverage. A schematic of the LSND detector is shown in Fig. 1. The tank is filled with 167 metric tons of liquid scintillator consisting of mineral oil and 0.031 g/l of b-PBD. The low scintillator concentration allows the detection of both Cerenkov light and scintillation light and yields a relatively long attenuation length of more than 20 m for wavelengths greater than 400 nm.[4] A typical 45 MeV electron created in the detector produces a total of $\sim$ 1500 photoelectrons, of which $\sim$ 280

photoelectrons are in the Cerenkov cone. The phototube time and pulse height signals are used to reconstruct the track with an average r.m.s. position resolution of $\sim$ 30 cm, an angular resolution of $\sim$ 12 degrees, and an energy resolution of $\sim$ 7%. The Cerenkov cone for relativistic particles and the time distribution of the light, which is broader for non-relativistic particles, give excellent particle identification. Surrounding the detector is a veto shield [5] which tags cosmic ray muons going through the detector.

DATA

The signature for a $\bar{\nu}_e$ interaction in the detector is the reaction $\bar{\nu}_e p \rightarrow e^+ n$ followed by $np \rightarrow d\gamma$ (2.2 MeV). A likelihood ratio, R, is employed to determine whether a γ is a 2.2 MeV photon correlated with a positron or is from an accidental coincidence. R is the likelihood that the γ is correlated, divided by the likelihood that it is accidental. R depends on the number of hit phototubes for the γ, the reconstructed distance between the positron and the γ, and the relative time between the γ and positron. Fig. 2 shows the expected R distribution for accidental photons and correlated photons. Fig. 3 shows the R distribution, beam on minus beam off, for events with positrons in the $36 < E < 60$ MeV energy range. The dashed histogram is the result of the R fit for events without a recoil neutron, and the solid histogram is the total fit, including events with a neutron. After subtracting the neutrino background with a recoil neutron there is a total excess of $54.8^{+18.5}_{-15.8} \pm 8.2$ events, which if due to neutrino oscillations corresponds to an oscillation probability of $(0.33^{+0.11}_{-0.10} \pm 0.05)\%$.

Fig. 4 shows the electron energy distribution, beam on minus beam off excess, for events (a) without a γ requirement and (b) events with an associated γ with $R > 30$. For this latter requirement, the total 2.2 MeV γ detection efficiency is 23% and the probability that an event has an accidental γ in coincidence is 0.6%. The dashed histogram shows the background from expected neutrino interactions. There are 22 events beam on in the $36 < E < 60$ MeV energy range and a total estimated background (beam off plus neutrino-induced background) of 4.6 ± 0.6 events. Table 1 lists the properties of these 22 events, while Table 2 shows the background estimate for events in the $36 < E_e < 60$ MeV energy range with $R \geq 0$ and $R > 30$. Fig. 5 shows the spatial distributions for the beam on-off excess events with $R \geq 0$ and $R > 30$. The probability that this excess is due to a statistical fluctuation is $< 10^{-7}$. If the observed excess is due to neutrino oscillations, Fig. 6 shows the allowed region (90% and 99% likelihood regions) of $\sin^2 2\theta$ vs Δm^2 from a maximum likelihood fit to the L/E distribution of the 22 beam on events. Some of the allowed region is excluded by the ongoing KARMEN experiment at ISIS,[6] the E776 experiment at BNL,[7] and the Bugey reactor experiment.[8]

CONCLUSION

In summary, the LSND experiment observes an excess of events with positrons in the $36 < E < 60$ MeV energy range that are correlated in time and space with a low energy γ. If the observed excess is interpreted as $\bar{\nu}_\mu \rightarrow \bar{\nu}_e$ oscillations, it corresponds to an oscillation probability of $(0.33^{+0.11}_{-0.10} \pm 0.05\%)$ for the allowed regions shown in Fig. 6. More data taking is planned for the experiment, and the performance of the detector is under continuous study. Both of these efforts are expected to improve the understanding of the phenomena described here. If neutrino oscillations have in fact been observed, then the minimal standard model would need to be modified and neutrinos would have mass sufficient to influence cosmology and the evolution of the universe.

REFERENCES

[1]The LSND Collaboration consists of the following people and institutions: K. McIlhany, I. Stancu, W. Strossman, G. J. VanDalen (Univ. of California, Riverside); W. Vernon (Univ. of California, San Diego and IIRPA); D. O. Caldwell, M. Gray, S. Yellin (Univ. of California, Santa Barbara); D. Smith, J, Waltz (Embry-Riddle Aeronautical Univ.); A. M. Eisner, Y-X. Wang (Univ. of California IIRPA); I. Cohen (Linfield College); R. L. Burman, J. B. Donahue, F. J. Federspiel, G. T. Garvey, W. C. Louis, G. B. Mills, V. Sandberg, R. Tayloe, D. H. White (Los Alamos National Laboratory); R. M. Gunasingha, R. Imlay, H. J. Kim, W. Metcalf (Louisiana State Univ.): K. Johnston (Louisiana Tech Univ.); B. D. Dieterle, R. A. Reeder (Univ. of New Mexico); A. Fazely (Southern Univ); C. Athnassopoulos, L. B. Auerbach, R. Majkic, J. Margulies, D. Works, Y. Xiao (Temple Univ.).

[2]C. Athanassopoulos *et. al.* , Phys. Rev. Lett. **75**, 2650 (1995).

[3]C. Athanassopoulos *et. al.* , submitted to Phys. Rev. C.

[4]R. A. Reeder *et. al.* , Nucl. Instrum. Methods A **334**, 353 (1993).

[5]J. J. Napolitano *et. al.* , Nucl. Instrum. Methods A **274**, 152 (1989).

[6]B. Bodmann *et. al.* , Phys. Lett. B **267**, 321 (1991); B. Bodmann *et. al.* , Phys. Lett. B **280**, 198 (1992); B. Zeitnitz *et. al.* , Prog. Part. Nucl. Phys., **32** 351 (1994).

[7]L. Borodovsky *et. al.* , Phys. Rev. Lett. **68**, 274 (1992).

[8]B. Achkar *et. al.* , Nucl. Phys. **B434**, 503 (1995).

TABLE I. The 22 beam-on events with $R > 30$ and energy in the $36 < E_e < 60$ MeV range. For each event is given the year recorded, energy, spatial position, and distance from the PMT surfaces.

Event	Year	E(MeV)	X(cm)	Y(cm)	Z(cm)	D(cm)
1	1993	47.6	-66	-84	-77	115
2	1993	51.1	56	-96	53	103
3	1994	40.1	-36	196	-203	53
4	1994	44.2	69	-146	153	53
5	1994	39.4	-169	96	-347	39
6	1994	36.3	-156	-79	-207	84
7	1994	52.9	21	106	71	143
8	1994	37.0	31	156	-105	93
9	1994	42.4	-14	-121	-239	78
10	1994	37.7	-91	119	209	109
11	1994	54.3	-91	191	269	47
12	1994	55.8	71	-99	-259	100
13	1994	43.8	6	211	173	38
14	1995	49.2	-184	10	58	75
15	1995	56.5	128	-150	199	49
16	1995	37.4	45	-92	-239	107I
17	1995	45.1	-186	105	-126	45
18	1995	46.7	179	-93	-108	57
19	1995	40.2	-37	-71	160	128
20	1995	45.9	-161	87	-337	49
21	1995	36.3	46	150	107	100
22	1995	37.6	-73	107	-257	129

TABLE II. A list of all backgrounds with the expected number of background events in the $36 < E_e < 60$ MeV energy range for $R \geq 0$ and $R > 30$. The neutrinos are from either π and μ decay at rest (DAR) or decay in flight (DIF). Also shown are the number of events expected for 100% $\bar{\nu}_\mu \rightarrow \bar{\nu}_e$ transmutation.

Background	Neutrino Source	Events with $R \geq 0$	Events with $R > 30$
Beam Off		146.5 ± 3.2	2.52 ± 0.42
Beam-Related Neutrons		< 0.7	< 0.1
$\bar{\nu}_e p \rightarrow e^+ n$	$\mu^- \rightarrow e^- \nu_\mu \bar{\nu}_e$ DAR	4.8 ± 1.0	1.10 ± 0.22
$\bar{\nu}_\mu p \rightarrow \mu^+ n$	$\pi^- \rightarrow \mu^- \bar{\nu}_\mu$ DIF	2.7 ± 1.3	0.62 ± 0.31
$\bar{\nu}_e p \rightarrow e^+ n$	$\pi \rightarrow e\nu$ and $\mu \rightarrow e\nu\bar{\nu}$ DIF	0.1 ± 0.1	0
Total with Neutrons		7.6 ± 1.6	1.72 ± 0.38
$\nu_\mu \mathrm{C} \rightarrow \mu^- X$	$\pi^+ \rightarrow \mu^+ \nu_\mu$ DIF	8.1 ± 4.0	0.05 ± 0.02
$\nu_e\ ^{12}C \rightarrow e^-\ ^{12}N$	$\mu^+ \rightarrow e^+ \bar{\nu}_\mu \nu_e$ DAR	20.1 ± 4.0	0.12 ± 0.02
$\nu_e\ ^{13}C \rightarrow e^-\ ^{13}N$	$\mu^+ \rightarrow e^+ \bar{\nu}_\mu \nu_e$ DAR	22.5 ± 4.5	0.14 ± 0.03
$\nu e \rightarrow \nu e$	$\mu^+ \rightarrow e^+ \bar{\nu}_\mu \nu_e$ DAR	12.0 ± 1.2	0.07 ± 0.01
$\nu e \rightarrow \nu e$	$\pi \rightarrow \mu \nu_\mu$ DIF	1.5 ± 0.3	0.01 ± 0.01
$\nu_e \mathrm{C} \rightarrow e^- X$	$\pi \rightarrow e \nu_e$ DAR	3.6 ± 0.7	0.02 ± 0.01
$\nu_\mu \mathrm{C} \rightarrow \pi X$	$\pi \rightarrow \mu \nu_\mu$ DIF	0.2 ± 0.1	0
$\nu_e \mathrm{C} \rightarrow e^- X$	$\pi \rightarrow e\nu$ and $\mu \rightarrow e\nu\bar{\nu}$ DIF	0.6 ± 0.1	0
Total without Neutrons		68.6 ± 7.4	0.41 ± 0.04
Grand Total		222.7 ± 8.2	4.65 ± 0.57
100% Transmutation	$\mu^+ \rightarrow e^+ \bar{\nu}_\mu \nu_e$ DAR	12500 ± 1250	2875 ± 345

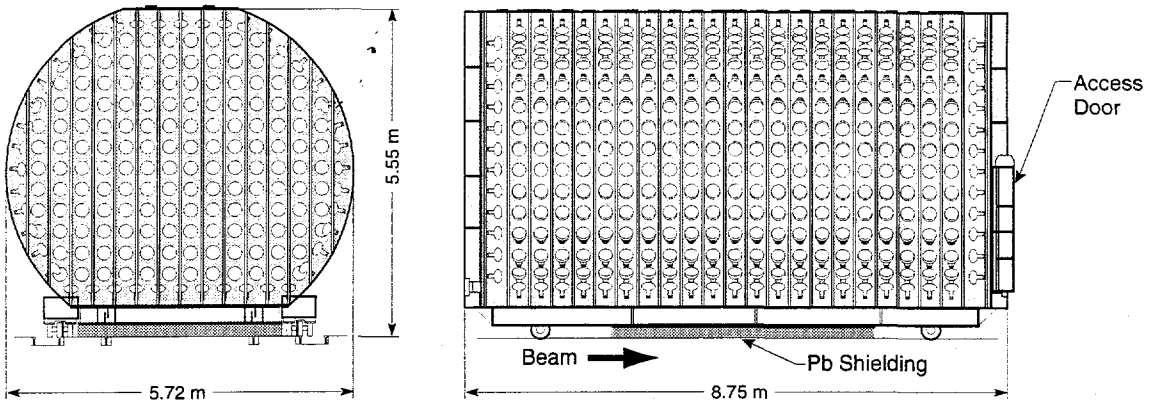

FIG. 1. A schematic of the LSND detector.

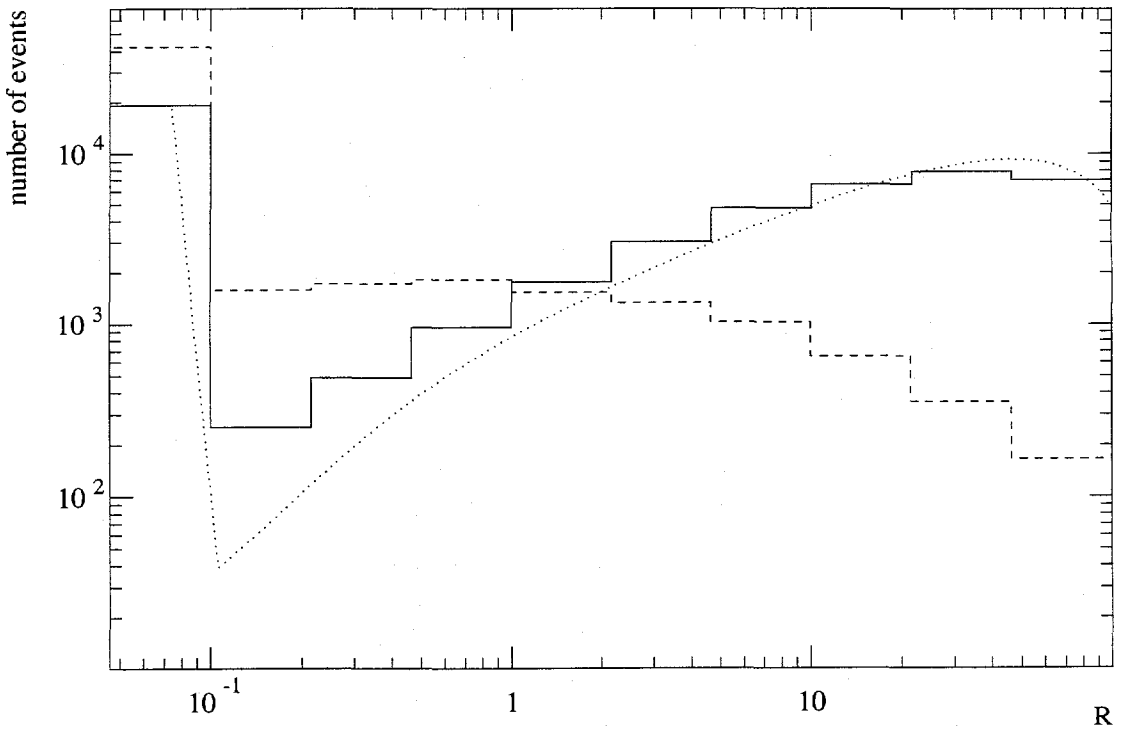

FIG. 2. Measured R distribution for events with the γ correlated (solid) and uncorrelated (dashed) with the primary event. The dotted curve is the Monte Carlo R distribution for events with the γ correlated.

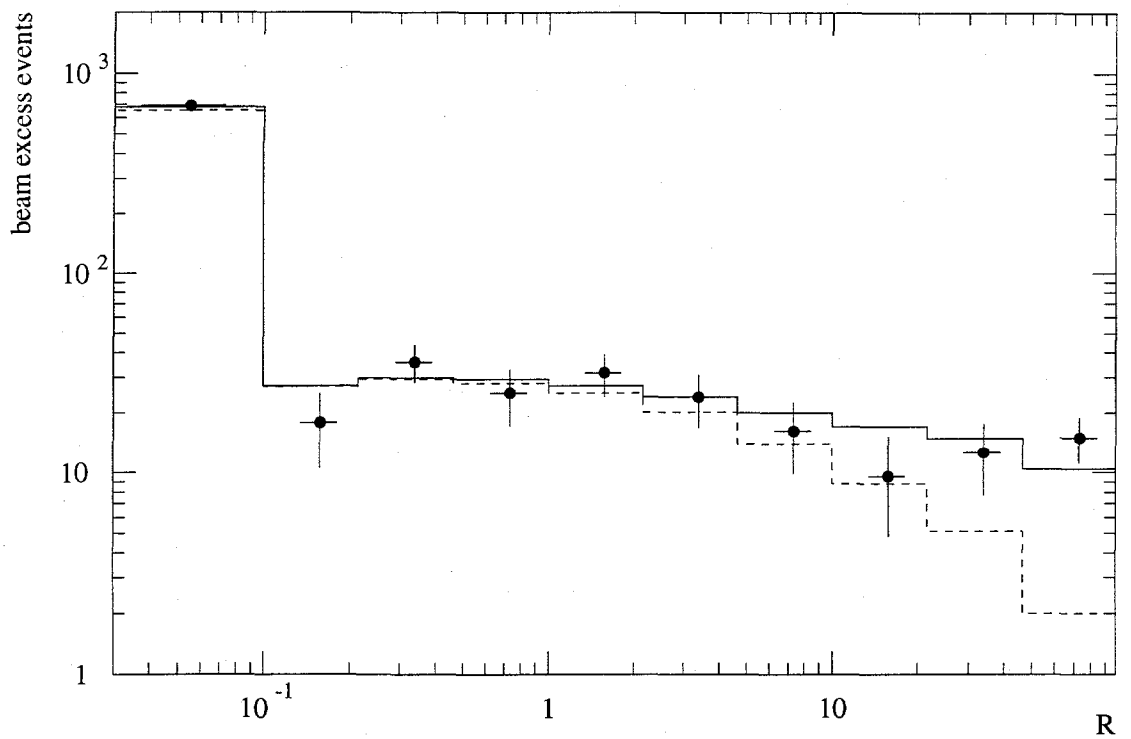

FIG. 3. The R distribution, beam on minus beam off excess, for events that have energies in the range $20 < E_e < 60$ MeV. The solid curve is the best fit to the data, while the dashed curve is the component of the fit with an uncorrelated γ.

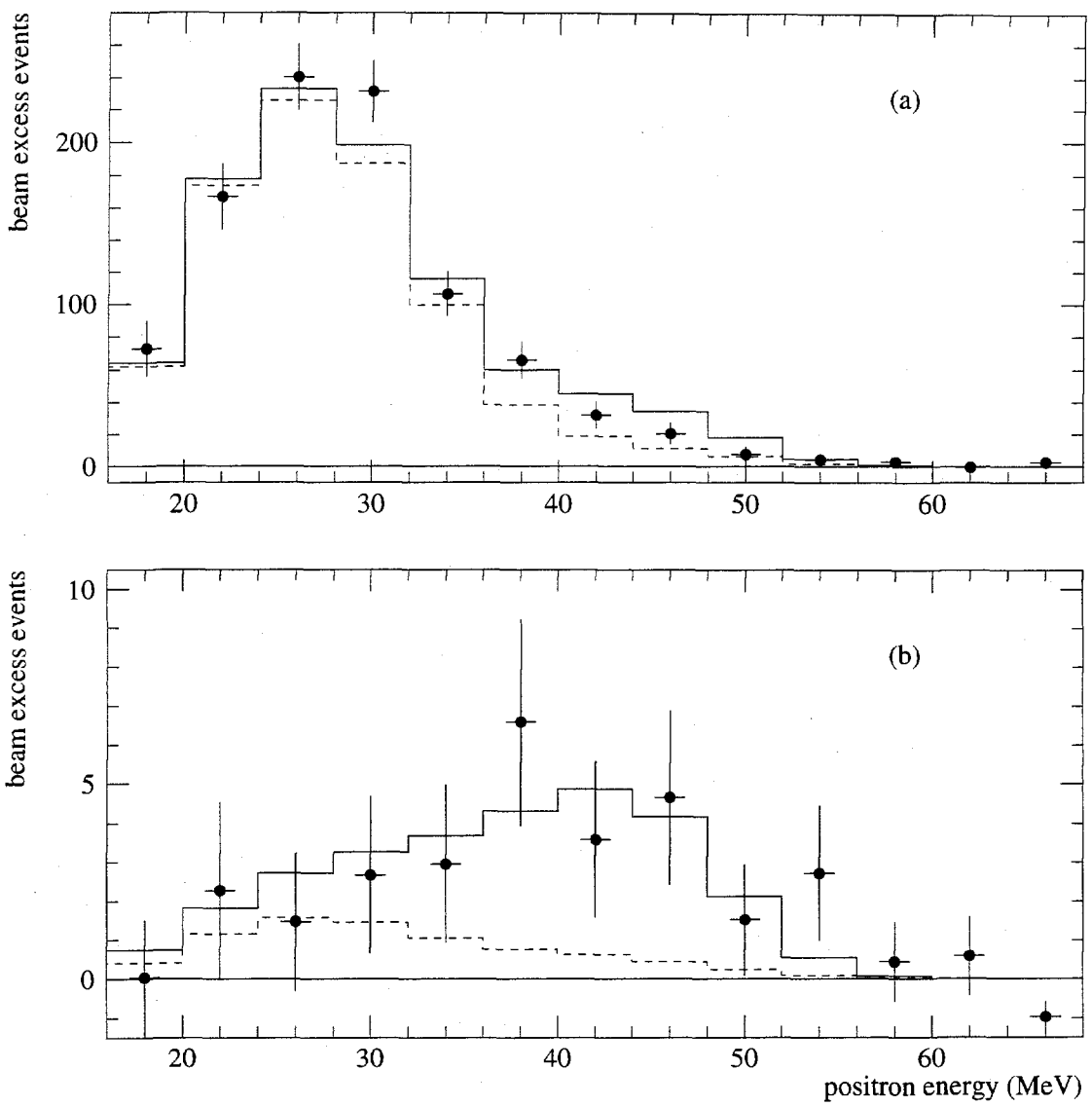

FIG. 4. The energy distribution for events with (a) $R \geq 0$ and (b) $R > 30$. Shown in the figure are the beam-excess data, estimated neutrino background (dashed), and expected distribution for neutrino oscillations at large Δm^2 plus estimated neutrino background (solid).

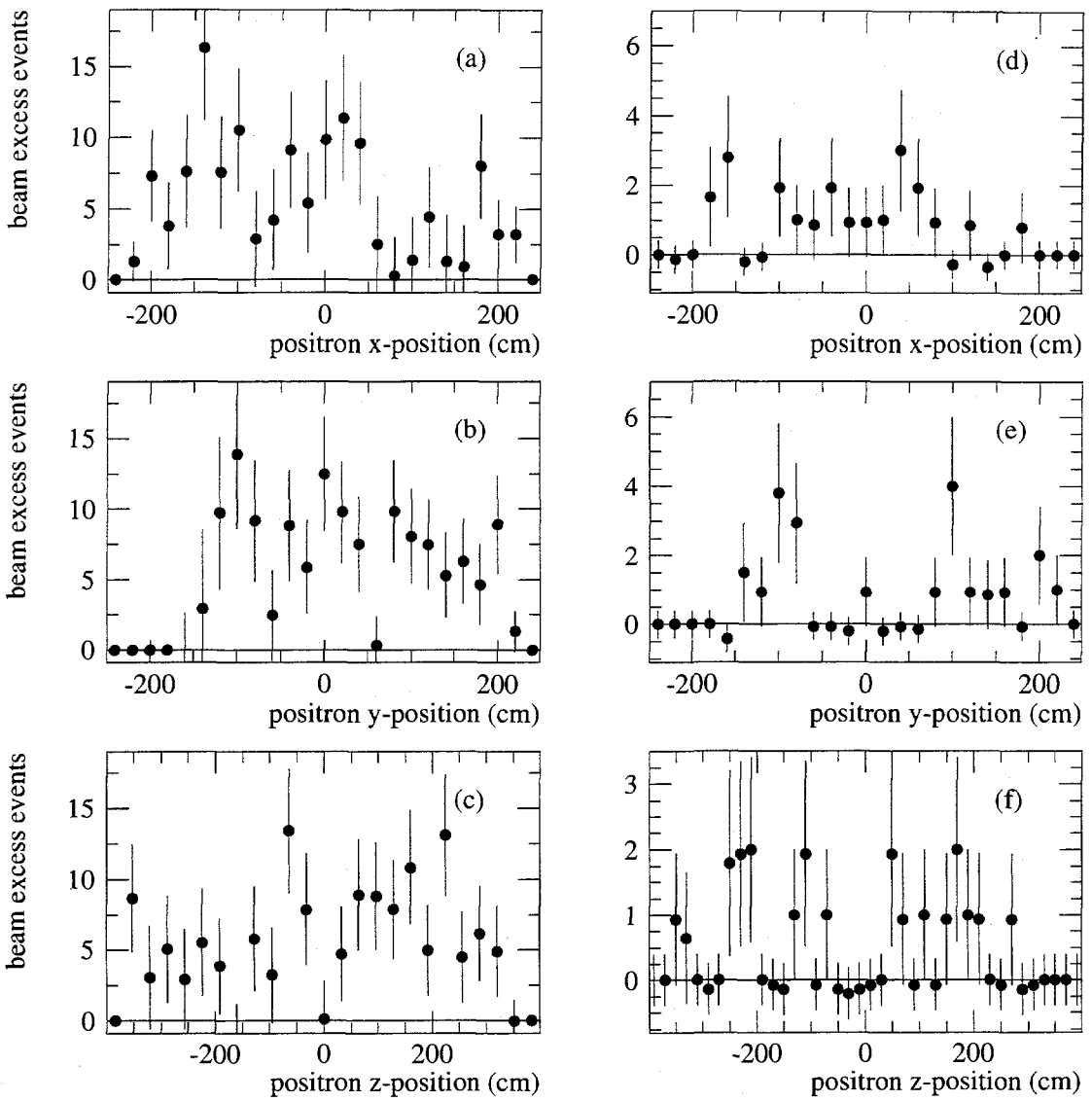

FIG. 5. The spatial distributions for beam-excess data events with $36 < E_e < 60$ MeV. (a) - (c) are for $R \geq 0$ and (d) - (f) are for $R > 30$.

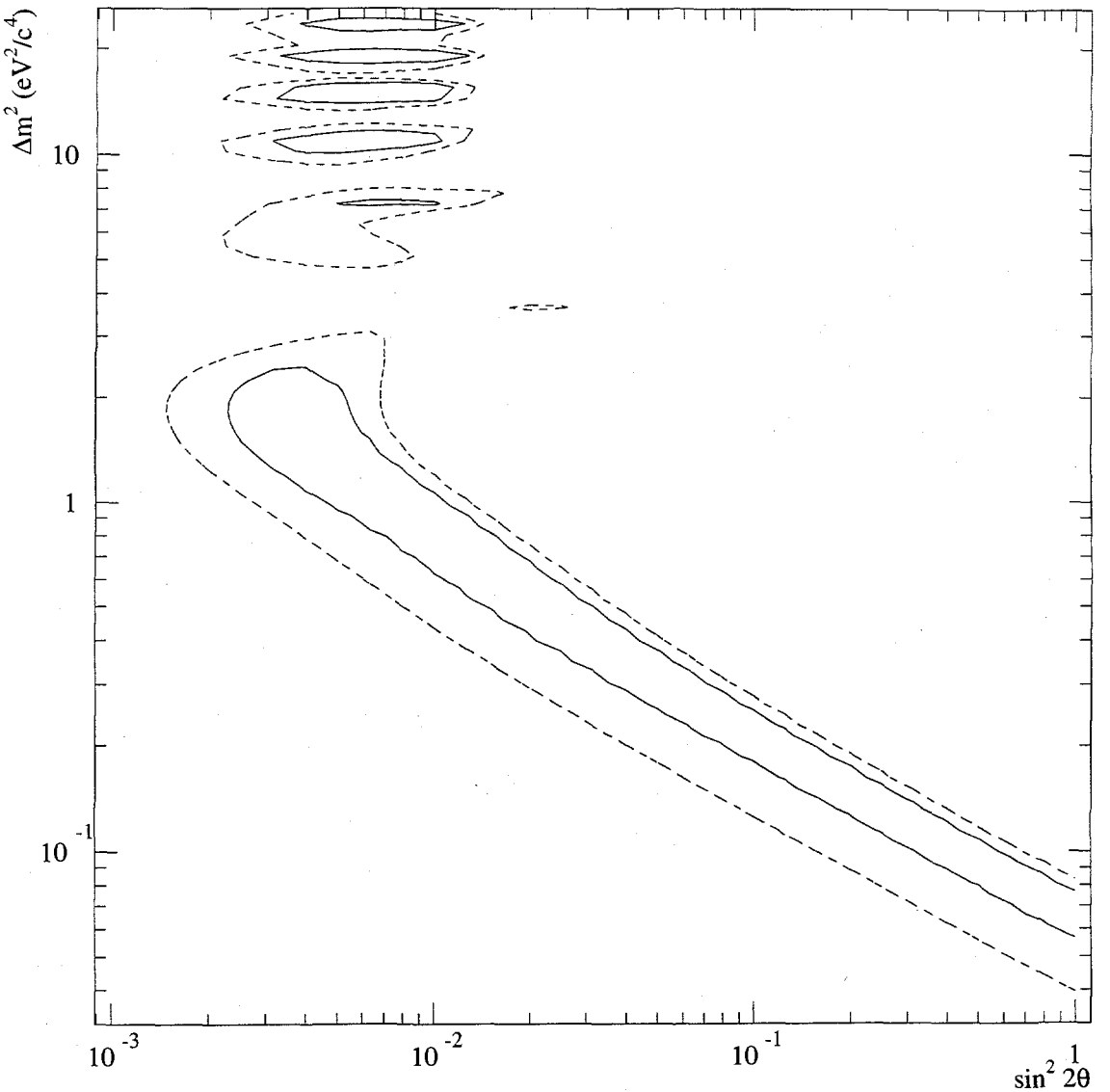

FIG. 6. Plot of the LSND Δm^2 *vs* $\sin^2 2\theta$ favored regions. They correspond to 90% and 99% likelihood regions after the inclusion of the effects of systematic errors.